LWT - Food Science and Technology 209 (2024) 116725

Contents lists available at ScienceDirect

LWT

journal homepage: www.elsevier.com/locate/lwt

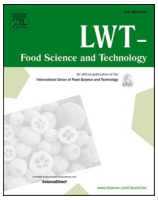

Fabrication and characterization of active gelatin-based films integrated with nanocellulose-stabilized Pickering emulsion containing *Oliveria Decumbens Vent.* essential oil

Hoda Fahim [a], Hadiseh Bagheri [b], Ali Motamedzadegan [a], Saeed Mirarab Razi [c], Ali Rashidinejad [d,*]

[a] Department of Food Science and Technology, Sari Agriculture Science and Natural Resources, Sari, Iran
[b] Department of Food Science and Technology, Sari Branch, Islamic Azad University, Sari, Iran
[c] Department of Food Science and Technology, Ferdowsi University of Mashhad, Mashhad, Iran
[d] Riddet Institute, Massey University, Private Bag 11 222, Palmerston North, New Zealand

ARTICLE INFO

Keywords:
Pickering emulsion
Nanocellulose
Oliveria decumbens vent essential oil
Active films

ABSTRACT

Stabilizing essential oils (EOs) within biodegradable matrices to create homogeneous and stable films with desirable properties is challenging due to the hydrophobic nature of EOs, which hinders their uniform infusion into the matrix. In this study, we investigated the feasibility of creating active films made of gelatin, infused with nanocellulose-stabilized Pickering emulsion (PE) containing *Oliveria Decumbens Vent.* essential oil (OEO). The Pickering emulsion effectively stabilized the 50% v/v of OEO, which was subsequently incorporated into a gelatin film at 0, 3, 5, 7, and 9% v/v, to produce active films. FTIR data showed that the OEO-PE was physically trapped in the film matrix through hydrogen bonds, which was also verified by SEM micrographs. The addition of OEO-PE notably changed the films' mechanical properties, leading to reduced tensile strength and enhanced elongation ($P < 0.05$) with no significant impact on their water vapor permeability. The incorporation of OEO endowed the film matrix with high antioxidant and antibacterial activity against *E. coli* and *S. aureus*. Thermal analysis using differential scanning calorimetry showed a 36–171 °C endothermic peak in all films, due to water evaporation and melting. The gelatin film containing 9% OEO-PE exhibited superior physical properties, enhanced water resistance, and excellent antibacterial and antioxidant activity.

1. Introduction

Currently, oil-based packaging materials, particularly single-use ones, are extensively utilized throughout the food supply chain to ensure food preservation and safety. However, due to their durability and non-biodegradability, these materials pose significant threats to the environment, polluting both land and sea. Consequently, numerous efforts have been made to mitigate the environmental pollution caused by plastic packaging, including the adoption of biopolymers as the primary material. Essentially, biodegradable biopolymers can effectively address pollution issues as they degrade more readily compared to plastics (Amin et al., 2022).

Various biopolymers have been used as film-packaging materials; e.g., gelatin, collagen, soy protein isolate, and starch (Cha & Chinnan, 2004). Gelatin is an animal-based biopolymer derived from animal connective tissues (Lu et al., 2022). Like other biopolymers, it possesses excellent film-forming properties. This is due to its ability to form a thin, continuous layer, a characteristic that is crucial for packaging films. However, its application is limited due to its poor mechanical and moisture barrier properties (Khan & Sadiq, 2021; Luo, Wu, Wang, & Yu, 2021). Scientists have made extensive efforts to overcome these drawbacks. These include using nanomaterials as fillers to enhance the mechanical properties, and incorporating various oils, including essential oils, to improve the barrier and hydrophobic properties of gelatin-based films (Atarés & Chiralt, 2016; Martelli-Tosi et al., 2018; Onyeaka et al., 2023).

Pickering emulsion films are a unique type of film that amalgamates all the previously mentioned properties. These films maximize the benefits of nanomaterials, which act as stabilizing agents, and essential oils, which serve as hydrophobic, antioxidant, and antimicrobial

* Corresponding author.
E-mail address: A.Rashidinejad@massey.ac.nz (A. Rashidinejad).

https://doi.org/10.1016/j.lwt.2024.116725
Received 2 July 2024; Received in revised form 26 August 2024; Accepted 4 September 2024
Available online 7 September 2024

components. Pickering emulsions represent a distinct class of emulsions, stabilized by colloidal solid particles instead of conventional emulsifiers (Berton-Carabin & Schroën, 2015).

Nanocellulose is a promising material for use as a Pickering agent. Cellulose is the most abundant biopolymer in the world and is commonly found in plants. Nanocellulose has the potential to be used as a reinforcing agent in the polymer matrix, thereby enhancing the mechanical and thermal properties of gelatin films. The presence of several hydroxyl groups on the surface of cellulose enables inter and intramolecular hydrogen bonds, which in turn provide a uniform dispersion in hydrophilic polymer matrices like gelatin (Onyeaka et al., 2023). In addition to its reinforcing application, it has been shown that cellulose nanocrystals can stabilize oils in the aqueous medium, as they are flexible enough to position at the interface of the oil/water droplet (Capron & Cathala, 2013).

Incorporating Pickering emulsions into the gelatin matrix can offer additional benefits, especially when essential oils are used as the oil fraction. Specifically, essential oils have demonstrated significant antioxidant and antimicrobial properties. When these oils are used as the oil fraction in Pickering emulsion-based films, the resulting packaging can be classified as active. A variety of essential oils, including clove, cinnamon, and thyme, have been incorporated into the film matrix to produce active packaging (Du et al., 2009; Hosseini, Razavi, & Mousavi, 2009).

Oliveria decumbens Vent belongs to the Apiaceae family, and has high antimicrobial and antioxidant activity (Habibollah Abbasi, Fahim, Mahboubi, & Tahmasbi, 2019; Esmaeili, Karami, & Maggi, 2018). Utilizing *Oliveria decumbens Vent* essential oil as an oil fraction of a nanocellulose Pickering emulsion, and incorporating it into a gelatin film matrix can be beneficial in two ways. First, nanocellulose, acting as a Pickering agent, can enhance the mechanical properties of the films. Second, the Pickering emulsion, which contains *Oliveria decumbens Vent* essential oil, imparts antimicrobial and antioxidant properties to the film matrix, thus creating active packaging. Accordingly, in this study, our focus was on utilizing nanocellulose as a Pickering agent. The aim was to stabilize the essential oil within an aqueous system by utilizing nanocellulose as a Pickering agent, where nanocellulose could be used as a Pickering agent to produce a Pickering emulsion. To verify emulsion production and stability, we aimed to assess optical microscopic images, stability over time, particle size, and zeta potential. Next, we aimed to integrate the fabricated emulsion into the film matrix, ensuring the creation of a homogeneous and uniform active film. We sought to harness the dual benefits of the cellulose Pickering emulsion; its antimicrobial properties and its reinforcing capabilities, and loading such an emulsion with *Oliveria decumbens* Vent essential oil. To our knowledge, this is the first instance of *Oliveria decumbens* Vent essential oil being used as a natural active agent in cellulose-based Pickering emulsion systems. Moreover, no prior studies have attempted to integrate such a system into a gelatin film matrix or assessed its potential bioactive functions. This research, therefore, presents a novel approach in this field.

2. Materials and methods

Gelatin, with a bloom number of 200, was purchased from Merck Chemical Co. (Darmstadt, Germany). Nanocellulose was extracted from medical-grade cotton wool (Negin Hydrophile Cotton, Iran). The essential oil of Oliveria decumbens Vent was procured from Tabib Daru Pharmaceutical Co. (Mashhad Ardehal- Kashan- Iran). Glycerol was obtained from Dr. Mojallali's Chemical Complex Company (Iran).

2.1. Nanocellulose preparation and characterization

Nanocellulose was extracted from cotton wool through acid hydrolysis, based on the method described by Pirich et al. (2019) with slight modifications. In brief, 50 g of chopped cotton wool was added to a 500 mL sulfuric acid solution (64% v/v) and stirred for 3.5 h at 55 °C. After the hydrolysis process, the solution was quenched with 10-fold distilled water. The solution was then centrifuged (Orum Tadjhiz, Iran) for 15 min at 2823 g to separate the cellulose particles from the acidic aqueous solution. The precipitates were retained, and the clear supernatant was discarded. This process was repeated several times until the supernatant became turbid. The milky supernatant was then placed into dialysis tubes (12000–14000 Da cut-off, Merck) and dialyzed against distilled water for a week at room temperature (25 °C), with the dialysis water being exchanged daily. Once the pH of the nanocellulose solution reached 5–6, the solution was treated with ultrasound (TOP Sonics, UP400, Iran) with a frequency of 20 kHz for 15 min at a power of 400 W to ensure full dispersion of the cellulose nanocrystals. The ultrasonicated solution was then centrifuged at 11292 g (PIT320 R, Famco, Iran) for 150 min, and the milky supernatant containing nanocrystalline celluloses, was collected and dried using an air-circulating oven at 40 °C for 24 h. To evaluate the particle size and zeta potential of nanocellulose, a 0.1% w/v nanocellulose solution in distilled water was prepared and analyzed using Dynamic Light Scattering (DLS; Nanotrac Wave 2, Microtrac, United States) (Hedjazi & Razavi, 2018).

2.2. Pickering emulsion (PE) preparation and characterization

Pickering emulsions were prepared with slight modifications based on the method reported by Saidane, Perrin, Cherhal, Guellec, and Capron (2016). In brief, nanocelluloses were dispersed in distilled water at a concentration of 1% w/v and sonicated for 2 min to ensure a complete and uniform dispersion of nanocellulose in the aqueous phase. Oliveria decumbens Vent essential oil (OEO) was added to the nanocellulose dispersion at a ratio of 50% v/v and homogenized using an ULTRA--TURRAX® homogenizer (IKA-T25 model, Staufen, Germany) at 15000 rpm for 5 min. The mixture was immediately transferred to a sonicator (UP400A model, Topsonic, Iran); the titanium probe of the sonicator was placed near the surface of the emulsion and sonicated for 5 min at 300 W (7 s on, 3 s off). The emulsions were placed in an ice bath during the homogenization and sonication processes to avoid the adverse effects of heat increase.

The average droplet diameter and zeta potential of the emulsions were analyzed using the method described by Hedjazi and Razavi (2018). 1 mL of each emulsion was diluted in 100 mL of distilled water and analyzed using Dynamic Light Scattering (Nanotrac Wave 2, Microtrac, United States).

2.3. Preparation of gelatin film loaded with pickering emulsion

Pickering emulsion films were prepared as follows. A 6% w/v gelatin solution was prepared by completely dissolving gelatin powder in distilled water at 50 °C. Glycerol was added to the gelatin solution at a ratio of 30% w/w based on the dry matter of the gelatin. Emulsions were added to the gelatin solution at concentrations of 0, 3, 5, 7, and 9% v/v, with the final film-forming solutions being 50 mL. A specified amount of the prepared Pickering emulsion films (25 mL) was poured into plastic Petri dishes with a diameter of 10 cm and placed in an air-circulating oven for 24 h at 35 °C. The dried films were peeled and stored in a desiccator containing conditioned silica gel at 48% relative humidity (RH) at room temperature before further analysis. All samples were conditioned at the mentioned RH% for three days before analysis (Almasi, Azizi, & Amjadi, 2020).

2.4. Fourier transform infrared (FTIR) spectroscopy

The FTIR spectra of the films were obtained by placing a piece of film under the single reflection crystal of an ATR device (Cary 630, Agilent Technologies Inc., Danbury, CT, USA). The spectra were recorded at a resolution of 1 cm^{-1} using a DTGS detector in the range of 600–4000 cm^{-1}.

2.5. Color analysis

The color of the film samples was analyzed using the Image Pardazesh device (IMG Pardazesh, Iran). This system comprised a digital camera (model ISH1000 Tucsen), an image-capturing box, and image analysis software (IMG Pardazesh CAM-System XI, Iran). Each sample was placed on a white background, and the L* a* b* parameters of at least 50 different points of each image were calculated using the ImageJ software (Tabaestani, Sedaghat, Pooya, & Alipour, 2013).

2.6. Film morphology

The surface morphology and cross-section of the films were visualized using scanning electron microscopy (SEM) at an acceleration voltage of 20 kV. The surface and fresh cut of the cross-section of the films were sputter-coated with gold. Cross-section images were captured at 500x, 1kx, and 2kx magnifications, while surface images were taken at 500x and 1kx magnifications (Hasanzati Rostami, Motamedzadegan, Hosseini, Rezaei, & Kamali, 2017).

2.7. Mechanical strength

The mechanical properties of the films were evaluated using a Koopa Universal Machine (TA model, Koopa, Iran), in accordance with the ASTM D882-97 standard (ASTM, 1999). Briefly, the samples were cut into rectangular shapes measuring 1 × 10 cm and conditioned at 55% RH and 25 °C for three days prior to testing. The samples were secured between grips with an initial distance of 40 mm, a trigger load of 5 g, and a crosshead speed of 1 mm/s.

2.8. Film solubility in water (FS)

The solubility of films in the water was measured using the method described by Habib Abbasi, Fahim, and Mahboubi (2021). The films were cut into pieces measuring 4 × 4 cm, accurately weighed, and placed in a circulating air oven at 105 °C for 24 h. The dried samples were weighed again and immersed in distilled water for 24 h; then, the mixture was passed through filter paper (Whatman No. 1). The filter papers were subsequently placed in the oven at 105 °C for 24 h and weighed once more. The solubility of the films was measured using the following formula:

$$FS\% = \frac{W_i - W_f}{W_i} \times 100 \quad \text{(Eq. 1)}$$

Where, W_i is the initial weight of dried film (g), and W_f is the weight of the dry insolubilized films.

2.9. Water vapor permeability (WVP)

The water vapor barrier properties of the films were measured using ASTM E96. Briefly, each sample was tightly sealed to the mouth of a cup (26 mm ID), which had been previously filled with dry silica gels. The cups were placed in a desiccator containing water at room temperature (ASTM-E96). The cups were weighed daily for 18 days, and the water vapor permeability (WVP) was measured using the following equation:

$$WVP = \frac{G}{t}\frac{x}{A\Delta p} \quad \text{(Eq. 2)}$$

Where, x represents the average film thickness (m) measured at least 5 points of the film spacemen. A is the exposure area of the film (m^2), $\frac{G}{t}$ is the slop of the weight gain curve, and $\Delta p = P_0(RH_1 - RH_2)$, where P_0 is the saturated water vapor pressure at the test temperature, and $(RH_1 - RH_2)$ refers to the real water pressure difference across the film.

2.10. Phenolic properties and antioxidant activity

An aliquot of the film (0.02 g) was mixed with 25 mL of methanol and stirred at room temperature for 30 min. It was then subjected to ultrasound at 200 W for 5 min. The supernatant was used for 2,2-diphenyl-1-picrylhydrazyl (DPPH), total phenol content, and ferric reducing antioxidant power (FRAP), and total phenol content (TPC) analyses as described by Tongnuanchan, Benjakul, and Prodpran (2012).

2.10.1. TPC assay

The total phenolic content of the film samples was measured using the method described by Chavoshi, Didar, Vazifedoost, Shahidi Noghabi, and Zendehdel (2022) with the Folin Ciocâlteu reagent. An aliquot of the extract (500 μL) from the solution prepared from the films was transferred to a test tube along with 2500 μl of Folin Ciocâlteu reagent. After resting for 5 min, 2000 μl of sodium carbonate (7.5%) was mixed into the solution, and then the film mixture was kept in a dark place for 40 min. The absorbance of the mixture was measured using a spectrophotometer at a wavelength of 760 nm. The absorbance of different concentrations of Gallic acid (25–400 μg/mL) was used as a standard to create a calibration curve. The total phenolic content was defined as mg of Gallic acid per g of film.

2.10.2. FRAP assay

The ability of OEO-PE films to reduce iron (III) was evaluated using the method described by Yıldırım, Mavi, and Kara (2001). Samples, each of 2.5 mL, were combined with an equal volume of phosphate buffer (0.2 M, pH 6.6) and potassium ferricyanide[1] (10 g/L). This mixture was then incubated at 50 °C for a duration of 30 min. Following this, 2.5 mL of trichloroacetic acid (100 g/L) was added to the solution, which was subsequently centrifuged for 10 min. The supernatant (2.5 mL) was then mixed with 2.5 mL of distilled water and 0.5 mL of Ferric chloride[2] (1 g/L). The absorbance of the samples was measured at a wavelength of 700 nm. It is important to note that a higher absorbance value indicates a greater reducing power.

2.10.3. DPPH assay

The film extract was added to 1 mL of a 0.1 mM DPPH solution. The resulting mixture was thoroughly mixed and then left in a dark room for 15 min. The light absorption of the samples was measured at 517 nm. Ascorbic acid solution and DPPH solvent (without the sample) were used as the control positive and control negative, respectively. These steps were also carried out on BHA, which served as a standard antioxidant (Tongnuanchan et al., 2012). The percentage of DPPH activity, also known as radical scavenging activity, was calculated using the following formula.

$$\text{Radical scavenging activity} = \left[\left(\frac{A_{control} - A_{sample}}{A_{control}}\right)\right] \times 100 \quad \text{(Eq. 3)}$$

Where, $A_{control}$ represents the absorbance of the control and A_{sample} represents the absorbance of the sample.

2.11. Antimicrobial activity

The film's antibacterial activity against *Escherichia coli* (ATCC 25,922) and *Staphylococcus aureus* (ATCC 25,923) was measured using the inhibition zone method, as described by Habib Abbasi et al. (2021) with slight modification. A fresh microbial solution of 100 μl, equivalent to 0.5 McFarland turbidity, was spread on Mueller Hinton agar. A well with a diameter of 9 mm was punched out on the agar plates, and 0.5 mL

[1] $K_3Fe(CN)_6$.
[2] $FeCl_3$.

of the film-forming solution was poured into it. The plates were then incubated for 24 h at 37 °C. An antibiotic disc (cefalexin) and a blank disk were used as positive and negative controls, respectively.

2.12. Thermal analysis

The thermal properties of the films were analyzed using Differential Scanning Calorimetry (400-Ci, Sanaf, Iran). Film specimens (~10 mg) were placed in an aluminum pan and heated from 25 to 250 °C at a rate of 10 °C/min under a nitrogen flow rate of 50 mL/min. An empty aluminum pan was used as a reference (Jamróz, Juszczak, & Kucharek, 2018).

2.13. Statistical analysis

A completely randomized design (CRD) was employed for the statistical analysis of results, and all experiments were conducted in triplicate (n = 3). The analysis of variance (ANOVA) was performed, and a mean comparison was conducted using the Duncan test. The significance level was set at $P < 0.05$. The results were analyzed using SPSS software (Version 16.0).

3. Results and discussion

3.1. Nanocellulose and pickering emulsion characterization

The analysis of nanocellulose revealed a size and zeta potential of 182.2 nm and −48.2 mV, respectively, confirming that acid hydrolysis of cotton can successfully produce nanocrystalline cellulose. These results align with the findings of other researchers who used sulfuric acid for hydrolysis (Jamróz et al., 2018; Wang et al., 2020; Wang et al., 2021). The size and surface charge of nanocellulose were 177.8 nm and −48.7, respectively, making them suitable as a Pickering agent for producing emulsions (Table 1). Our observed results confirmed that 1% w/v nanocellulose can effectively stabilize OEO in the system, with the emulsion remaining completely stable for 30 days at room temperature (25 °C) (Fig. 1A-B). During the ultrasound process, small OEO droplets were produced, and nanocellulose present in the medium covered the OEO, effectively acting as a physical barrier against droplet coalescence in the emulsion system (Fig. 1C) (Souza, Ferreira, Aguilar, Zanata, & Rosa, 2021). The droplet size of emulsions containing 50% OEO was 1441.2 nm, and the zeta potential was −19.1 mV (Table 1). In addition to the barrier behavior of nanocellulose, the stabilization mechanism of the emulsion could be described by electrostatic and steric repulsion between droplets (emulsion zeta potential results) (Souza et al., 2021). These researchers prepared nanocellulose-based Pickering emulsions using cinnamon essential oil. They found that emulsions containing 30% oil, with a zeta potential around −29 mV, exhibited a low creaming index and were electrostatically stabilized. Additionally, emulsions with 20% oil had a zeta potential of −15 mV and remained stable for a month, indicating steric stabilization.

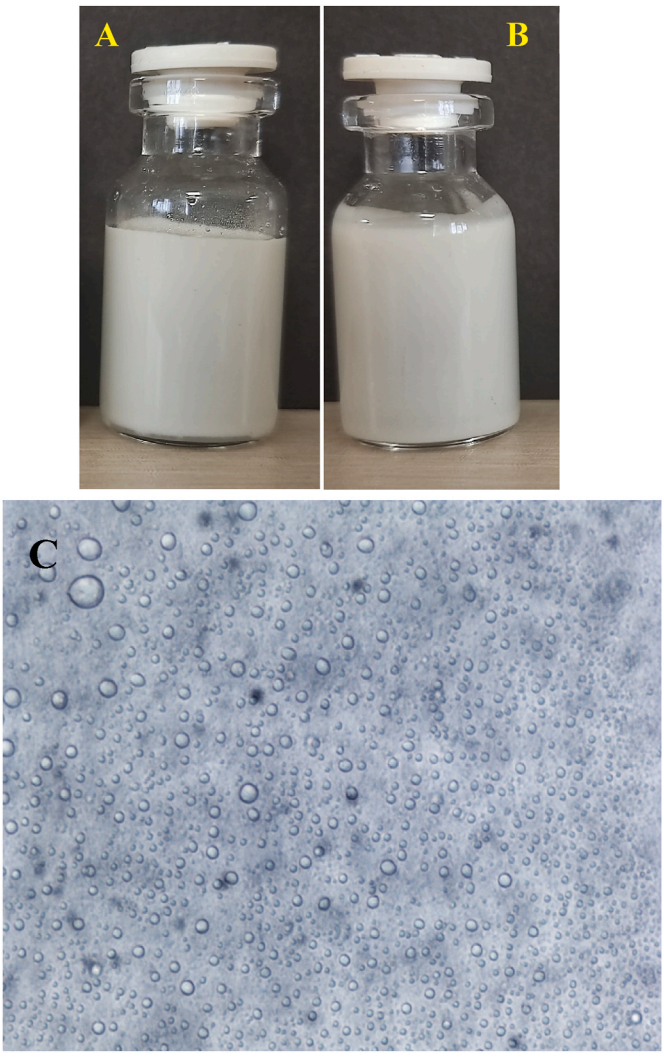

Fig. 1. A: Freshly prepared *Oliveria Decumbens Vent.* essential oil Pickering emulsion (OEO-PE), B: Physically-stable formulation of OEO-PE after 1 month of storage, and C: Optical microscopy image of the fresh OEO-PE at 40x magnitude.

Table 1
Color parameters, solubility in water, water vapor permeability (WVP), and mechanical properties of the gelatin films containing 0, 3, 5, 7, and 9% *Oliveria Decumbens Vent.* essential oil.

OEO-PE	Film characteristics								
	Color parameters			Mechanical properties					
	L*	a*	b*	Elongation (%)	Tensile strength (MPa)	FS (%)	WVP (gr/kpa.day.m)	Size (nm)	Zeta potential
0%	70.94 ± 3.95^{a}	−2.74 ± 0.02^{a}	8.98 ± 0.67^{c}	30.24 ± 4.69^{c}	22.26 ± 6.61^{b}	83.71 ± 0.49^{a}	0.14 ± 0.02^{a}	–	–
3%	62 ± 1.69^{b}	−2.08 ± 0.2^{b}	18.9 ± 2.06^{b}	26.36 ± 4.45^{c}	38.25 ± 3.87^{a}	73.49 ± 0.82^{b}	0.16 ± 0.03^{a}	–	–
5%	65.7 ± 0.73^{b}	−2.13 ± 0.01^{b}	19.71 ± 0.45^{b}	27.56 ± 3.61^{c}	24.12 ± 4.99^{b}	71.93 ± 0.52^{b}	0.1 ± 0.03^{a}	–	–
7%	63.85 ± 1.06^{b}	−2.09 ± 0.24^{b}	20.64 ± 0.41^{b}	47.69 ± 8.43^{b}	20.83 ± 2.66^{b}	69.61 ± 0.51^{c}	0.15 ± 0.02^{a}	–	–
9%	64.18 ± 0.64^{b}	−2.35 ± 0.12^{b}	29.03 ± 0.06^{a}	67.33±8^{a}	19.21 ± 4.93^{b}	66.021 ± 0.97^{d}	0.17 ± 0.002^{a}	–	–
CNC	–	–	–	–	–	-	-	177.8	−48.7
PE	–	–	–	–	–	–	–	1441.2	−19.1

3.2. Film characterization

3.2.1. FTIR spectroscopy

Fig. 2A and B represent the FTIR spectra of gelatin films with varying concentrations of OEO-PE. The prominent peaks associated with gelatin molecules, which are consistent across all samples, include a stretching absorption peak at 3293 cm^{-1}, attributed to N-H amide type A, and two absorption peaks at approximately 1540 cm^{-1} and 1635 cm^{-1} assigned to amide II and amide I, respectively. Additionally, a peak at 1235 cm^{-1} was observed, which was attributed to amide bands (amide III) with C-H_2 of glycine and proline side chains of gelatin. Amides are functional and characteristic groups found in proteins, such as gelatin. In FTIR spectra, these functional groups commonly appear in four regions known as amide A, amide I, amide II, and amide III (Wahyuningtyas, Jadid, Burhan, & Atmaja, 2019). Habib Abbasi et al. (2021) reported similar peaks for gelatin films at 3291, 1527, 1621, and 1221 cm^{-1} for the above-mentioned amide. Other research on gelatin films also confirmed these prominent peaks for gelatin (Roy & Rhim, 2021; Shahiri Tabarestani, Sedaghat, Jahanshahi, Motamedzadegan, & Mohebbi, 2017). A sharp peak was also noted at 1631 cm^{-1}, related to the O-H vibration of absorbed water.

In addition to peaks attributed to gelatin functional groups, the FTIR spectra also revealed prominent peaks associated with nanocellulose. A strong peak at 1032 cm^{-1} is attributed to the stretching vibration of C-O groups, i.e., asymmetric stretching vibrations of pyranose rings and bridge C-O-C bands. Additionally, a peak at 1388 cm^{-1} is attributed to C-H and C-O vibrations found in the polysaccharides. Wulandari, Rochliadi, and Arcana (2016) reported two peaks at 1060 and 1382 cm^{-1} corresponded to cellulose functional groups; i.e., C-O-C pyranose ring and C-H and C-O of polysaccharide rings, respectively which was following our results. In addition, peaks between 2900 cm^{-1} and 2950 cm^{-1}, which are attributed to the C-H stretching vibrations of the cellulose, are also present. All these peaks are associated with the presence of nanocellulose of PE in the film matrix (Foo, Tan, Wu, Chan, & Chew, 2017; Wulandari et al., 2016).

As seen in Fig. 2, the presence of OEO in the film matrix did not produce any new peaks, but the intensity of the O-H and C-H stretching peaks increased with a higher amount of OEO-PE. This might be due to the presence of larger quantities of phenolic compounds such as Thymol and Carvacrol, confirming the existence of OEO in the system and its physical entrapment within the film matrix. In a study on nanofiber starches loaded with carvacrol, Fonseca et al. (2019) reported that the incorporation of carvacrol in the fibers did not produce a new band in the FTIR spectra which were similar to our findings. These authors claimed that EO in the nanofibers was mixed physically without a chemical reaction. Physical entrapment of EO in the polymer matrix with no new characteristic bands was also reported by other researchers (Barzegar et al., 2021; Keawchaoon & Yoksan, 2011).

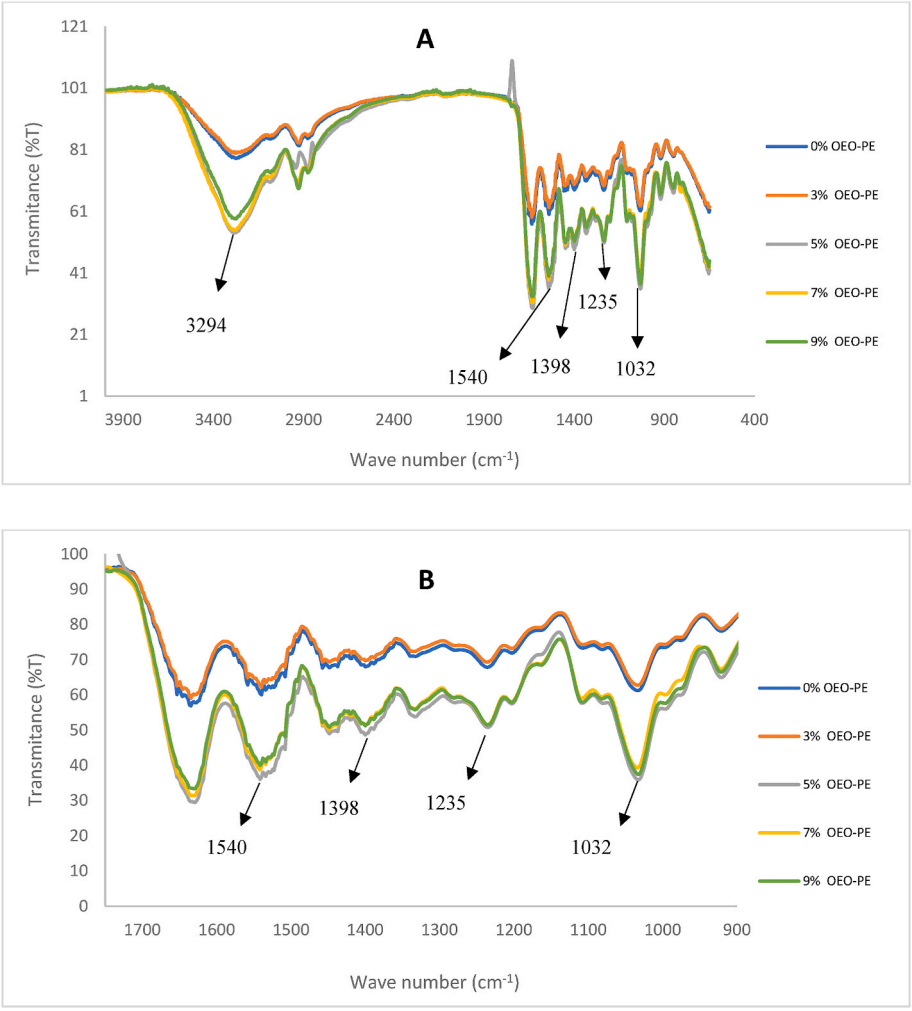

Fig. 2. Fourier transform infrared (FTIR) spectra of gelatin films containing 0, 3, 5, 7, and 9% *Oliveria Decumbens Vent.* essential oil Pickering emulsion (OEO-PE) at a range of A) 650-4000 cm^{-1} and B) 900- 1800 cm^{-1}.

3.2.2. Color characteristics

Color analysis of OEO-PE films and the physical appearance of films are presented in Table 1 and Fig. 3, respectively. The results showed that the lightness of the films significantly decreased after incorporating OEO-PE ($P < 0.05$). This could be due to changes in light scattering as a result of the presence of emulsion droplets distributed in the film matrix. In addition, the a* parameter, which reflects the greenness of films, also decreased after incorporating OEO-PEs. The a* value of the 0% OEO-PE film was -2.74 ± 0.02, which significantly decreased to a range of -2.08 ± 0.2 to -2.35 ± 0.12 for the 3% and the 9% OEO-PE films, respectively. The b* parameter, representing the yellowness or blueness of the films, significantly increased after adding OEO-PEs ($P < 0.05$). The yellowness of the control film was 8.98 ± 0.67, which significantly increased to 29.03 ± 0.06 for the 9% OEO-PE film ($P < 0.05$). This suggests that incorporating OEO in the film matrix led to a deeper yellowish color, which may be due to the natural yellow color of the essential oil from *Oliveria Decumbens Vent*. The essential oil has a yellow, light brown color; therefore, incorporating it in the film matrix led to a yellowish appearance of the film as reflected in the results of the b* parameter (Table 1) and confirmed by the visual color change depicted in Fig. 3. This figure was used to illustrate the visual appearance, including transparency and color. Films containing varying concentrations of OEO-PE were placed on a white background with a black printed letter, and their images were compared. The color change and increase in the b* parameter as a result of incorporating EO in the film matrix were also reported by Dai et al. (2023), who confirmed that the color of films was visually influenced by the EO portion in the film and films with a higher amount of cinnamon essential oil had a more yellowish color and a higher b* parameter. Similar results were also reported in a study done by Liu et al. (2022) on cinnamon essential oil Pickering emulsions in chitosan composite films.

3.2.3. Film morphology

The surface and cross-section morphologies of the films are depicted in Fig. 4A–F. The control film, composed of pure gelatin, exhibited a relatively smooth and uniform surface without any inhomogeneity or cracks. Additionally, the cross-section of this film showed only a few cracks across the film. Other studies on the surface morphology of pure gelatin films have confirmed that gelatin provides a compact and uniform structure (Habib Abbasi et al., 2021; Dai et al., 2023). In contrast, adding OEO-PE into the gelatin matrix resulted in a relatively non-uniform surface, as shown in Fig. 4C–F. The surface of the films displayed the formation of certain curved surfaces, specifically for films with 9% OEO-PEs (Fig. 4E–F), implying the presence of sub-surface EO in the film structure. This is typical behavior of films containing high levels of Pickering emulsion (Dammak, Lourenço, & do Amaral Sobral, 2019). However, the surface uniformity of OEO-PE films was sufficient to conclude that the film-forming emulsions were highly stable and that creaming and coalescence had not occurred during the drying process (Pereda, Aranguren, & Marcovich, 2010; Shi et al., 2016).

The investigation of a cross-section of OEO-PE films revealed a heterogeneous and porous structure; some grainy particles were present, which might represent emulsion droplets. Emulsion droplets at the cross-section of the matrix did not show any aggregation and were uniformly dispersed (Fig. 4C–F). This uniform distribution can be attributed to the use of nanocellulose with negative charges that prevent droplet aggregation or coagulation (Khalil et al., 2017). In addition, some micro-structured sized holes throughout the cross-section of OEO-PE films, especially in films containing higher amounts of EO-PEs, could be due to the presence of essential oil droplets in the matrix that interrupt chain entanglement of gelatin molecules, giving rise to a more disordered and porous network (Dammak et al., 2019; Pastor, Sánchez-González, Chiralt, Cháfer, & González-Martínez, 2013).

3.2.4. Mechanical properties

Mechanical property parameters, including tensile strength (TS) and elongation (%E) of films, are presented in Table 1. The results showed that incorporating OEO-PEs at 7% and 9% concentrations into the gelatin matrix could significantly increase %E compared to a pure gelatin film. The control and 3% OEO-PEs films had the lowest %E of

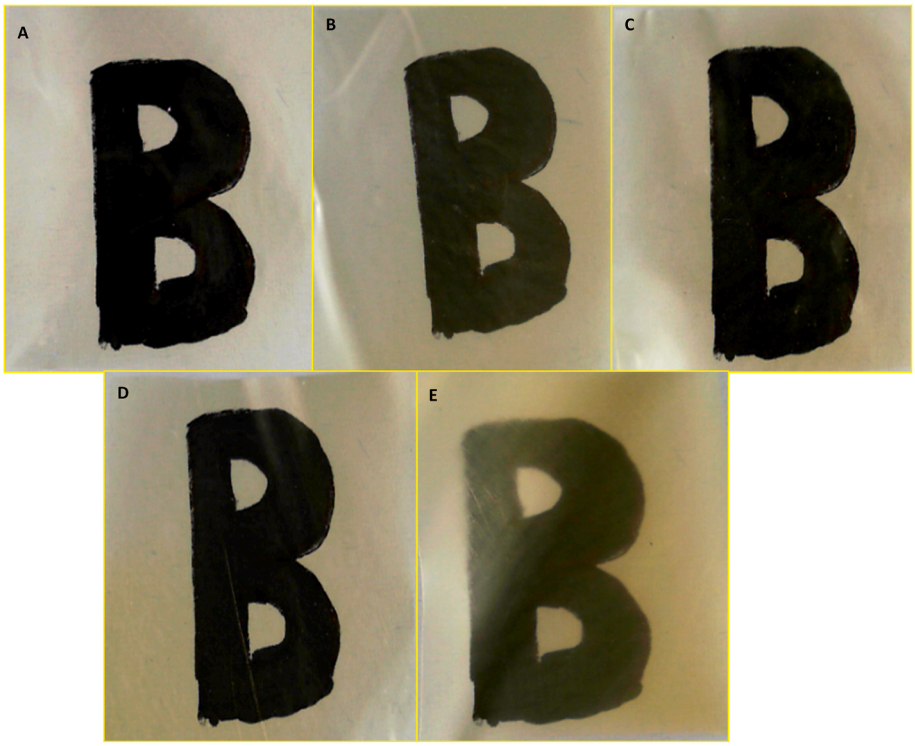

Fig. 3. The physical appearance of films with different concentrations of *Oliveria Decumbens Vent.* essential oil Pickering emulsion (OEO-PE). A: Pure gelatin film, B: 3% OEO-PE film, C: 5% OEO-PE film, D: 7% OEO-PE film, E: 9% OEO-PE film.

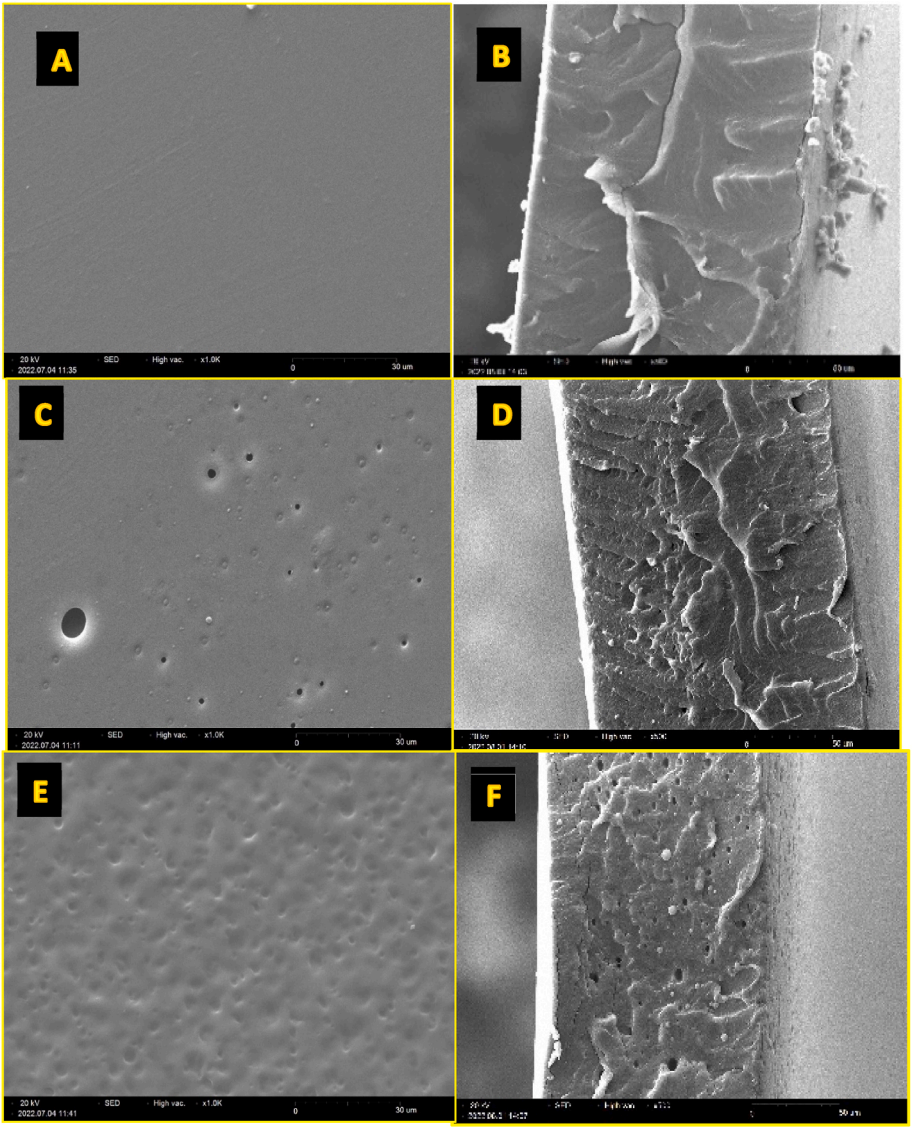

Fig. 4. Scanning electron micrographs of the films with different concentrations of *Oliveria Decumbens Vent*. essential oil Pickering emulsion (OEO-PE). A and B: Surface and cross-section of the pure gelatin film, C and D: Surface and cross-section of the 3% OEO-PE film; E and F: Surface and cross-section of the 9% OEO-PE film, respectively.

30.24 ± 4.69 and 26.36 ± 4.45, respectively, with no significant differences between them. However, as the concentration of OEO-PE increased to 9% in the film, %E rose to 67.33 ± 8%. On the contrary, OEO-PE content was not significant in the TS of the films except for the 3% OEO-PEs. The highest TS was 38.25 ± 3.87 MPa for the 3% OEO-PEs film, whereas it was significantly lower in films containing 0, 5, 7, and 9% OEO-PEs. This suggests that the emulsion primarily enhanced the extensibility of the films, while its effect on the TS parameter was insignificant.

In general, the glycerol used in the film formulation acted as a lubricant between gelatin chains and enhanced film elasticity. However, the results showed that OEO-PEs may also have a plasticizing effect. In this regard, Dammak et al. (2019) and Robledo et al. (2018) reported that nanoemulsions in the film matrix could act as a plasticizer, thereby affecting the mechanical properties of films. Another explanation for this behavior is that the presence of emulsion droplets may reduce chain entanglement and enhance their molecular mobility. More precisely, emulsion droplets in the microstructure of the films could prevent the formation of intermolecular junctions, leading to a decrease in forces between chains and reducing the strength of the films (Dammak et al., 2019; Pereda et al., 2010; Shi et al., 2016). In addition, Shi et al. (2016) suggested that the increase in %E of films could be associated with the deformability of the lipidic nature of EO, as lipid droplets can easily deform during tensile tension, which aligns with our results. The results of the mechanical properties of the films were confirmed by the SEM images (Fig. 4) as these images depicted the presence of OEO-PE droplets and also tiny holes in the cross-section of the films which could influence the mechanical properties (see Fig. 4C–F).

3.2.5. *Water solubility of the film (FS)*

The results of the water solubility of films are shown in Table 1. FS is a vital parameter of biodegradable films since they are used as a protective layer on food and may have direct contact with food ingredients (Shakila, Jeevithan, Varatharajakumar, Jeyasekaran, & Sukumar, 2012). The pure gelatin film showed significantly higher water solubility than other films ($P < 0.05$). On the contrary, introducing OEO-PEs into the gelatin matrix significantly reduced their solubility, specifically in films with a higher portion of OEO-PEs. As shown in Table 1, the highest solubility was 83.71 ± 0.49% for the pure gelatin film, which was similar to the results of gelatin film solubility reported in previous

studies (Ahmad & Sarbon, 2021; Peña, De La Caba, Eceiza, Ruseckaite, & Mondragon, 2010; Shakila et al., 2012).

The water solubility of the gelatin film is mainly governed by the hydrophilic nature of gelatin chains, so water molecules can form hydrogen bonds with the chain, leading to the high solubility of the pure gelatin film in water. However, the decreased water solubility by adding OEO-PEs to the matrix film can be explained by the probable interaction between nanocellulose (as wall material of Pickering emulsion droplets) and gelatin. Nanocellulose is a hydrocolloid with no solubility in water but has free hydroxyl groups that can form hydrogen bonds (Rogovina, Aleksanyan, Prut, & Gorenberg, 2013). This means that nanocellulose can form hydrogen bonds with gelatin chains, so the water uptake by proteins may decrease since the water molecule can't disrupt the previously formed hydrogen bonds between nanocellulose and gelatin. They can't penetrate the gelatin film matrix, swell, and dissolve it (Ahmad & Sarbon, 2021). In this regard, Oyeoka, Ewulonu, Nwuzor, Obele, and Nwabanne (2021) reported that adding nanocellulose at 5 and 10% w/w to PVA-Gelatin films could decrease %FS to 63 and 60%, respectively which was similar to our results. Oyeoka et al. (2021) claimed that the decrease in FS was mainly due to the formation of strong hydrogen bonding between the film matrix and nanocellulose, consequently decreasing the film's water sensitivity and restricting the film matrix's dissolution in the water medium.

In addition to nanocellulose, the presence of OEO in the Pickering emulsion has also affected the FS. The structure of OEO is essentially hydrophobic, which means that it forms hydrophobic interactions with the helical structure of the gelatin and alters its solubility. More precisely, the non-polar components of the essential oil can interact with the hydrophobic domains of gelatin, enhancing the hydrophobicity of the final film. Peña et al. (2010) reported that adding tannin to the gelatin matrix decreased its solubility, similar to our results. Relatedly, Ahmad, Benjakul, Prodpran, and Agustini (2012) reported that incorporating EO with a hydrophobic structure into gelatin films decreased solubility. The change in gelatin structure due to the presence of OEO in the film was confirmed by the thermal analysis of the films, which will be discussed further in the next section.

3.2.6. Water vapor permeability

The water barrier property of films is a critical parameter for biodegradable packaging films, as they are a determining factor in preventing moisture reabsorption, oxidation, and deterioration of food ingredients (Fan et al., 2023). In general, the water permeation across films follows three steps: first, sorption and solubilization of water molecules on the film surface that come into contact with the higher water vapor concentration. Second, water molecules diffuse throughout the polymer matrix due to the concentration gradient. Third, evaporation of water molecules from the side that comes into contact with a lower water vapor concentration (Dammak et al., 2019).

As shown in Table 1, the vapor permeability of films did not significantly change by adding OEO-PEs into the gelatin matrix. Many studies reported that incorporating Pickering emulsion into film matrices decreased the barrier properties of films mainly due to an increase in the oil or essential oil droplets in the film structure (Dai et al., 2023; Dammak et al., 2019) or an increase in the migration path of water vapor (Fan et al., 2023; Shen et al., 2021). However, our findings showed that an increase in OEO as a hydrophobic component did not work in favor of decreasing WVP as in many previous studies. This may be explained by the higher number of cracks and holes formed after incorporating different levels of OEO-PEs (as depicted in Fig. 4C–F). In this regard, Abdulkhani, Hosseinzadeh, Ashori, Dadashi, and Takzare (2014) and Habib Abbasi et al. (2021) reported a slight increase in WVP after adding Nanocrystalline cellulose and electrospun cellulose acetate, respectively, which is inconsistent with our findings. In addition, Roy and Rhim (2021) reported that integrating Pickering emulsions of clove EO stabilized with nanocellulose in the gelatin/agar films increased WVP due to the high amount of nanocellulose in the matrix and its free hydroxyl groups that enhance water attraction. In our study, OEO-PEs did not increase WVP like the work of Roy and Rhim (2021), which may be due to the presence of OEO and its hydrophobic nature, which somehow could combat the tiny cracks and micrometer holes in the structure (Fig. 4C–F).

3.2.7. Phenolic properties and antioxidant activity

The phenolic properties and antioxidant activity of active films were measured by different tests, including TPC, FRAP, and DPPH assays, as presented in Table 2. The results confirmed that incorporated OEO contained high phenolic compounds. The film containing 0% OEO exhibited no TPC, whereas by incorporating OEO, the TPC values in the films increased from 5.62 ± 0.05 to 15.1 ± 0.2 for the 3% and 9% OEO-PE films, respectively. In previous studies, it was confirmed that *Oliveria Decumbens Vent.* EO had high phenolic content, and the main components were thymol, Carvacrol, p-cymene, and γ-terpinene (Alizadeh Behbahani, Tabatabaei Yazdi, Vasiee, & Mortazavi, 2018; Esmaeili et al., 2018; Karami, Kavoosi, & Maggi, 2019; Saidi, 2014). Based on Esmaeili et al. (2018), OEO has 14.8–16.7 mg GAE/g dry weight at different phenological stages, stages of plant growth, similar to our results (15.1 ± 0.2 for the 9% OEO-PE film). On the other hand, the high phenolic content of films positively correlated with the higher antioxidant activity of the OEO (Table 2). More precisely, the antioxidant activity of phenolic compounds is primarily due to their redox properties, which allow them to absorb or neutralize free radicals, act as a metal chelator, quench singlet or triplet oxygen (i.e., phenolic ring), which can donate hydrogen from the hydroxyl groups (Adilah, Jamilah, & Hanani, 2018; Javanmardi, Stushnoff, Locke, & Vivanco, 2003).

Aligned with the TPC results, the findings of the DPPH and FRAP assays, presented in Table 2, showed that as the OEO-PE concentration increased from 3% to 9%, the %RSA and FRAP increased prominently ($P < 0.05$). Both DPPH and FRAP assay results were in firm accordance with OEO's high phenolic content results (Table 2). In spite of phenolic content, DPPH scavenging activity might be related to flavonoid compounds in OEO (Mirahmad et al., 2024). Previous studies on active films containing EO have reported high antioxidant activity. For example, Malihi, Danafar, and Moosavi-nasab (2022) reported that the antioxidant activity of gelatin films containing OEO was enhanced by increasing the essential oil from 1% to 3%. These researchers reported a 71.18% DPPH value for a film with 3% essential oil. They concluded that the high antioxidant activity of the active film corresponds to its high phenolic content, which aligns with our results. In another study conducted by Nikravan, Maktabi, Ghaderi Ghahfarrokhi, and Mahmoodi Sourestani (2021), OEO, which was used to produce nanoemulsion, demonstrated excellent antioxidant activity. They also reported that utilization of OEO as an active agent was limited due to its low solubility in water, low stability, and high volatility. Therefore, emulsification would be a promising method to increase its stability. Aligned with their reports, and to overcome the destabilization of OEO in the film matrix, we successfully used nanocellulose to emulsify and stabilize OEO in the aqueous medium of the gelatin solution.

Our finding showed that cellulose, as a Pickering agent, could successfully stabilize OEO and allow us to incorporate it into the film matrix without phase separation (as depicted in Figs. 1–3). As a result, we could utilize OEO's high antioxidant and antimicrobial properties in the active films.

3.2.8. Antimicrobial activity

The antibacterial results of the active films, as presented in Table 2 and Fig. 5, were obtained using the agar well diffusion method. In general, our antimicrobial results aligned with antioxidant findings that confirmed the biological activity of the phenolic contents of the OEO. The antimicrobial results demonstrated that the control films had no antibacterial effect. However, the inhibition zones against *E. coli* and *S. aureus* were 13.93 ± 0.32 mm and 15.21 ± 0.5 mm, respectively, for the 3% OEO-PE films. Remarkably, these zones significantly increased to

Table 2
Antibacterial, antioxidant, and thermal properties of gelatin films containing 0, 3, 5, 7, and 9% *Oliveria Decumbens Vent.* essential oil.

	Antioxidant activity			Inhibition zone (mm)		*Thermal properties*	
	Total phenolic content (mg/mL)	FRAP (mg/mL)	DPPH (%)	*E. coli*	*S. auers*	Tm (°C)	ΔH (J/g)
0% OEO-PE	0^{e}	0.019 ± 0.008^{e}	3.47 ± 0.02^{e}	0^{d}	0^{d}	112.35	87.64
3% EO-PE	5.62 ± 0.05^{d}	0.27 ± 0.02^{d}	71.06 ± 0.07^{d}	13.93 ± 0.32^{c}	15.21 ± 0.5^{c}	107.2	82.6025
5% EO-PE	10.69 ± 0.11^{c}	0.47 ± 0.04^{c}	76.8 ± 0.28^{c}	14.65 ± 0.5^{c}	16.22 ± 0.96^{c}	109.6	57.745
7% EO-PE	12.48 ± 0.37^{b}	0.58 ± 0.02^{b}	81.87 ± 0.33^{b}	23.69 ± 0.81^{b}	28.19 ± 0.62^{b}	100.2	56.01
9% EO-PE	15.1 ± 0.2^{a}	0.66 ± 0.03^{a}	85.89 ± 0.35^{a}	33.75 ± 0.35^{a}	38.21 ± 0.76^{a}	88.25	56.57

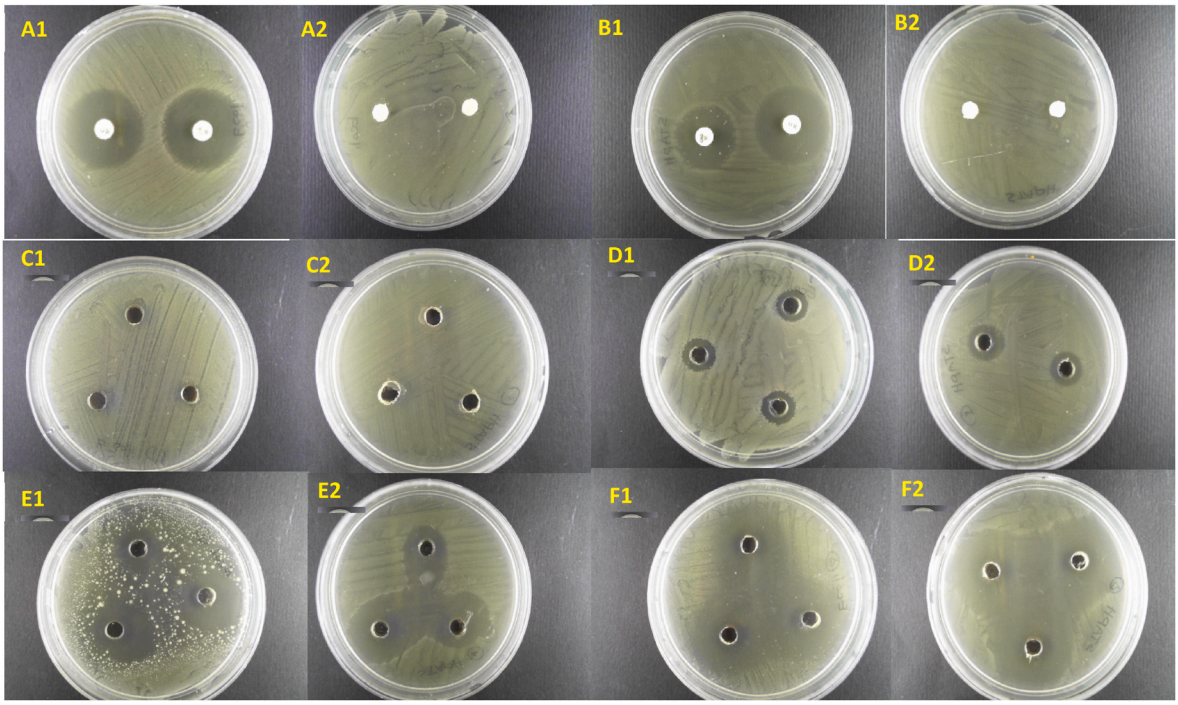

Fig. 5. Inhibition zones of various *Oliveria Decumbens Vent.* essential oil Pickering emulsion (OEO-PE) films. A1 and A2: Control+ and control-against *E. coli*, respectively; B1 and B2: Control+ and control-against *S. aureus*, respectively; C1 and C2: the 0% OEO-PE film against *E. coli* and *S. aureus*, respectively; D1 and D2: the 3% OEO-PE film against *E. coli* and *S. aureus*, respectively; E1 and E2: the 5% OEO-PE film against *E. coli* and *S. aureus*, respectively; F1 and F2: the 9% OEO-PE film against *E. coli* and *S. aureus*, respectively.

33.75 ± 0.35 mm and 38.21 ± 0.76 mm, respectively, for the 9% OEO-PE films. In addition, all films showed a more inhibitory effect on gram-positive bacteria, which aligns with previous studies on OEO. This may be due to the structure of bacterial walls. Gram-negative bacteria have an inner peptidoglycan layer and outer lipopolysaccharide membrane, while the walls of gram-positive bacteria consist only of a peptidoglycan layer, making them more susceptible to antibacterial agents (Abbasi et al., 2021; Malihi et al., 2022; Nikravan et al., 2021).

The antimicrobial activity of OEO may be due to its main constituents (i.e., bioactive compunds). OEO is rich in phenolics and terpenes, and the mechanism of action of these components is primarily due to interaction and consequently disruption of the bacterial membrane, increasing its permeability. For instance, carvacrol, dominantly present in the OEO, contains a phenolic OH group, which can transit through the bacterial plasma membrane, bind ATP molecules or cations like K^{+}, transport them out of the bacterial cell, and then disrupt bacterial homeostasis. Thymol, as one of the main bioactive constituents of OEO, on the other hand, can integrate into the polar-head region of the lipid layer, influencing the structural unity and fluidity of the membrane. In addition, this ingredient can bind membrane and periplasmic space proteins via hydrogen bonding and hydrophobic interactions, decreasing the bacterial response to antibacterial agents (Álvarez-Martínez, Barrajón-Catalán, Herranz-López, & Micol, 2021). Given that the OEO used in the film matrix in the curretn research consists of the same phenolic composition, pronounced antibacterial efficiency against the studied bacterial strains was anticipated (Fig. 5).

3.2.9. Thermal analysis

The thermal parameters and thermograms of OEO-PE films are presented in Table 2 and Fig. 6, respectively. All films exhibited similar thermal behavior and showed a distinct endothermic peak at 36–171 °C, which corresponded to the desorption of water and essential oil trapped in the OEO-PE and film matrix. This peak might also overlap with other processes, such as the melting of gelatin peptides (Rivero, Garcia, & Pinotti, 2010). The apex of this peak was 112.35 ± 1.2 °C for the 0% OEO-PE film (i.e., control film), which significantly shifted to lower temperatures of 88.25 ± 0.35 °C for the 9% OEO-PE film ($P < 0.05$). This result may be attributed to the presence of OEO and cellulose in the film matrix that changes the hydrogen bonding between polymer chains and alters their overall mobility (Kilinc, Ocak, & Özdestan-Ocak, 2021). In this regard, Tongnuanchan, Benjakul, Prodpran, Pisuchpen, and Osako (2016) reported that hydrophobic substances like fats, oils, or essential oils could slightly decrease the endothermic peak of gelatin films. These substances in polymer-based films could act as a plasticizer, disrupting intra and intermolecular interactions of protein chains, leading to a loosening of its structure. The results of these researchers were in accordance with our findings. In addition, the plasticizing effect of OEO was concluded based on our DSC results, evidenced by a

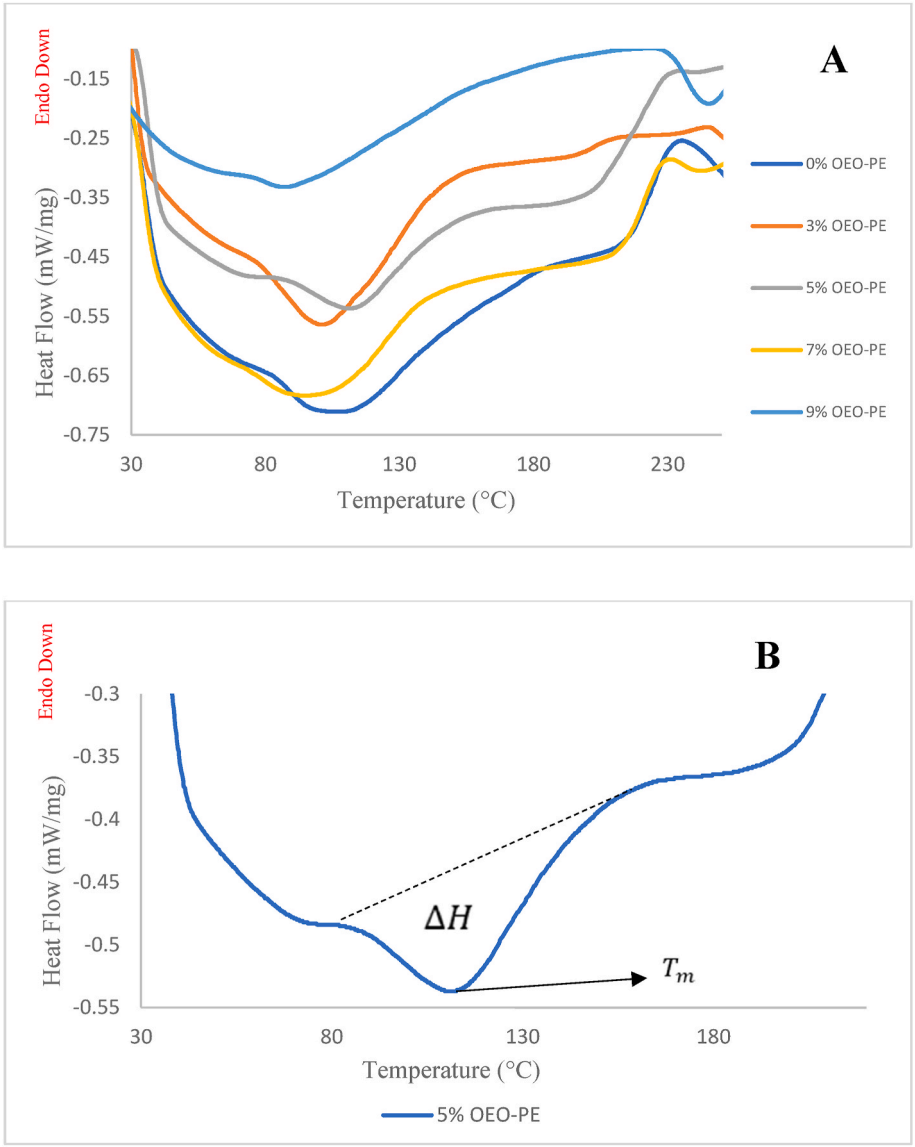

Fig. 6. Thermograms of gelatin films containing 0, 3, 5, 7, and 9% *Oliveria Decumbens Vent.* oil essential Pickering emulsion (OEO-PE; A), and thermograms of gelatin films containing 5% OEO-PE to represent the T_m and ΔH area (B).

decrease in the mechanical strength of films (Table 1).

Additionally, the enthalpy, or the area under the first peak, showed a decreasing trend with an increase in OEO-PE from 0 to 9%. Generally, the enthalpy of the peaks represents the amount of energy needed to evaporate water or OEO in the films (Fahim, Motamedzadegan, Farahmandfar, & Ghaffari Khaligh, 2023). Therefore, the more water or EO absorbed in the films results in higher enthalpy. The ΔH results for the 0% and 3% OEO-PE films were 87.64 ± 0.63 and 82.6 ± 0.73 J/g, respectively, which was higher than those for other samples with higher OEO-Pes; i.e., 56.57 J/g for the 9% OEO-PE film.

Gelatin has a hydrophilic nature, and the presence of water and glycerol as a plasticizer affected the thermal properties of films. Both increased water content, consequently causing a higher integration area. Contrarily, when the portion of OEO-PE into the matrix increased from 0 to 9%, the ΔH declined from 87.64 to 56.57 J/g, possibly due to two reasons. First, introducing OEO-PE in the film matrix caused new hydrogen and hydrophobic bonding between cellulose/OEO and gelatin chains, avoiding hydrogen bonds between water and gelatin, thereby decreasing the bonded water in the films. This means that although a portion of the water in the film matrix was replaced by OEO, due to the lower heat capacity of the OEO compared to water, less energy was needed to evaporate in films with higher OEO-PE content which consequently decreased its ΔHs (Kilinc et al., 2021; Peña et al., 2010; Tongnuanchan et al., 2016).

The second reason could be due to the structure of OEO. In other words, the decreased ΔH with the incorporation of PE in the film matrix could be the result of changes in the chain mobility of the gelatin polymer matrix. OEO-PE can disrupt the ordered molecular structure of the gelatin chains, forming a less-arranged structure that requires lower enthalpy for disruption of inter-chain interaction in the film matrix (as evidenced by SEM images and mechanical properties of films in Fig. 4 and Table 1, respectively). This finding follows the results of Tongnuanchan et al. (2016), who reported that the enthalpy of gelatin films decreased after incorporating EO. Similar results were also reported by Peña et al. (2010) and Kilinc et al. (2021).

4. Conclusions

Nanocellulose, extracted from cotton wool, successfully stabilized OEO, producing a stable Pickering emulsion. This Pickering emulsion was subsequently introduced into the gelatin matrix, resulting in a homogeneous, active film. The inclusion of OEO-PE in the film

significantly modified mechanical properties, such as tensile strength and elongation. The films turned yellow after the addition of OEO-PE, attributable to the presence of OEO. The TPC, DPPH, and FRAP analyses confirmed that all gelatin films manufactured in this study exhibited high antioxidant activity. Furthermore, the inhibition zone test results demonstrated that the films possessed significant antibacterial activity against *E. coli* and *S. aureus*. Both the antioxidant and antimicrobial activities of the films increased with the OEO-PE content. Thermal analysis of the films revealed that all films had an endothermic peak associated with the evaporation of water and OEO from the film matrix, which overlapped with the melting points. Therefore, stabilizing hydrophobic EO in the hydrophilic gelatin film matrix through the Pickering emulsion approach could be a promising method to enhance the mechanical, antimicrobial, and antioxidant activities of gelatin films. Our findings suggest that OEO-PE films can be successfully used as an inner active layer in food packaging, as they exhibit low solubility and can simultaneously prevent or retard microbial growth and oxidation in packaged foods. This is particularly important for foods with high-fat content and neutral pH.

CRediT authorship contribution statement

Hoda Fahim: Writing – original draft, Software, Resources, Project administration, Methodology, Investigation, Formal analysis, Data curation, Conceptualization. **Hadiseh Bagheri:** Writing – original draft, Software, Methodology, Data curation, Conceptualization. **Ali Motamedzadegan:** Writing – review & editing, Supervision, Resources, Project administration, Funding acquisition, Conceptualization. **Saeed Mirarab Razi:** Writing – review & editing, Validation, Supervision, Conceptualization. **Ali Rashidinejad:** Writing – review & editing, Validation, Conceptualization.

Declaration of competing interest

The authors declare that there is no conflict of interest for this work.

Data availability

Data will be made available on request.

References

Abbasi, H., Fahim, H., & Mahboubi, M. (2021). Fabrication and characterization of composite film based on gelatin and electrospun cellulose acetate fibers incorporating essential oil. *Journal of Food Measurement and Characterization, 15*(2), 2108–2118.

Abbasi, H., Fahim, H., Mahboubi, M., & Tahmasbi, N. (2019). Antibacterial properties and stability of emulsions containing Cuminum cyminum and Oliveria decumbens Vent. essential oils prepared by ultrasound. *Journal of food science and technology (Iran), 16*(87), 41–51.

Abdulkhani, A., Hosseinzadeh, J., Ashori, A., Dadashi, S., & Takzare, Z. (2014). Preparation and characterization of modified cellulose nanofibers reinforced polylactic acid nanocomposite. *Polymer Testing, 35*, 73–79.

Adilah, Z. M., Jamilah, B., & Hanani, Z. N. (2018). Functional and antioxidant properties of protein-based films incorporated with mango kernel extract for active packaging. *Food Hydrocolloids, 74*, 207–218.

Ahmad, M., Benjakul, S., Prodpran, T., & Agustini, T. W. (2012). Physico-mechanical and antimicrobial properties of gelatin film from the skin of unicorn leatherjacket incorporated with essential oils. *Food Hydrocolloids, 28*(1), 189–199.

Ahmad, A. A., & Sarbon, N. M. (2021). A comparative study: Physical, mechanical and antibacterial properties of bio-composite gelatin films as influenced by chitosan and zinc oxide nanoparticles incorporation. *Food Bioscience, 43*, Article 101250.

Alizadeh Behbahani, B., Tabatabaei Yazdi, F., Vasiee, A., & Mortazavi, S. A. (2018). Oliveria decumbens essential oil: Chemical compositions and antimicrobial activity against the growth of some clinical and standard strains causing infection. *Microbial Pathogenesis, 114*, 449–452.

Almasi, H., Azizi, S., & Amjadi, S. (2020). Development and characterization of pectin films activated by nanoemulsion and Pickering emulsion stabilized marjoram (Origanum majorana L.) essential oil. *Food Hydrocolloids, 99*, Article 105338.

Álvarez-Martínez, F. J., Barrajón-Catalán, E., Herranz-López, M., & Micol, V. (2021). Antibacterial plant compounds, extracts and essential oils: An updated review on their effects and putative mechanisms of action. *Phytomedicine, 90*, Article 153626.

Amin, U., Khan, M. K. I., Maan, A. A., Nazir, A., Riaz, S., Khan, M. U., … Lorenzo, J. M. (2022). Biodegradable active, intelligent, and smart packaging materials for food applications. *Food Packaging and Shelf Life, 33*, Article 100903.

ASTM. (1999). Standard test methods for tensile properties of thin plastic sheeting. D882-97. *Annual Book of ASTM Standards*, 163–171. Philadelphia, Pa.: ASTM Intl.

ASTM-E96. Standard test methods for water vapor transmission of materials. ASTM International: West, Conshohocken, PA, Vol. 96.

Atarés, L., & Chiralt, A. (2016). Essential oils as additives in biodegradable films and coatings for active food packaging. *Trends in Food Science & Technology, 48*, 51–62.

Barzegar, S., Zare, M. R., Shojaei, F., Zareshahrabadi, Z., Koohi-Hosseinabadi, O., Saharkhiz, M. J., et al. (2021). Core-shell chitosan/PVA-based nanofibrous scaffolds loaded with Satureja mutica or Oliveria decumbens essential oils as enhanced antimicrobial wound dressing. *International Journal of Pharmaceutics, 597*, Article 120288.

Berton-Carabin, C. C., & Schroën, K. (2015). Pickering emulsions for food applications: Background, trends, and challenges. *Annual Review of Food Science and Technology, 6*, 263–297.

Capron, I., & Cathala, B. (2013). Surfactant-free high internal phase emulsions stabilized by cellulose nanocrystals. *Biomacromolecules, 14*(2), 291–296.

Cha, D. S., & Chinnan, M. S. (2004). Biopolymer-based antimicrobial packaging: A review. *Critical Reviews in Food Science and Nutrition, 44*(4), 223–237.

Chavoshi, F., Didar, Z., Vazifedoost, M., Shahidi Noghabi, M., & Zendehdel, A. (2022). P syllium seed gum films loading Oliveria decumbens essential oil encapsulated in nanoliposomes: Preparation and characterization. *Journal of Food Measurement and Characterization, 16*(6), 4318–4330.

Dai, H., Chen, Y., Chen, H., Fu, Y., Ma, L., Wang, H., et al. (2023). Gelatin films functionalized by lignocellulose nanocrystals-tannic acid stabilized Pickering emulsions: Influence of cinnamon essential oil. *Food Chemistry, 401*, Article 134154.

Dammak, I., Lourenço, R. V., & do Amaral Sobral, P. J. (2019). Active gelatin films incorporated with Pickering emulsions encapsulating hesperidin: Preparation and physicochemical characterization. *Journal of Food Engineering, 240*, 9–20.

Du, W. X., Olsen, C., Avena-Bustillos, R., McHugh, T., Levin, C., & Friedman, M. (2009). Effects of allspice, cinnamon, and clove bud essential oils in edible apple films on physical properties and antimicrobial activities. *Journal of Food Science, 74*(7), M372–M378.

Esmaeili, H., Karami, A., & Maggi, F. (2018). Essential oil composition, total phenolic and flavonoids contents, and antioxidant activity of Oliveria decumbens Vent. (Apiaceae) at different phenological stages. *Journal of Cleaner Production, 198*, 91–95.

Fahim, H., Motamedzadegan, A., Farahmandfar, R., & Ghaffari Khaligh, N. (2023). A comparative study of the surface modification of cellulose using glutaric anhydride and succinic anhydride through a greener technique. *Cellulose*, 1–15.

Fan, S., Wang, D., Wen, X., Li, X., Fang, F., Richel, A., et al. (2023). Incorporation of cinnamon essential oil-loaded Pickering emulsion for improving antimicrobial properties and control release of chitosan/gelatin films. *Food Hydrocolloids, 138*, Article 108438.

Fonseca, L. M., dos Santos Cruxen, C. E., Bruni, G. P., Fiorentini, Â. M., da Rosa Zavareze, E., Lim, L.-T., et al. (2019). Development of antimicrobial and antioxidant electrospun soluble potato starch nanofibers loaded with carvacrol. *International Journal of Biological Macromolecules, 139*, 1182–1190.

Foo, M. L., Tan, K. W., Wu, T. Y., Chan, E. S., & Chew, I. M. (2017). A characteristic study of nanocrystalline cellulose and its potential in forming Pickering emulsion. *Chemical Engineering Transactions, 60*, 97–102.

Hasanzati Rostami, A., Motamedzadegan, A., Hosseini, S. E., Rezaei, M., & Kamali, A. (2017). Evaluation of plasticizing and antioxidant properties of silver carp protein hydrolysates in fish gelatin film. *Journal of Aquatic Food Product Technology, 26*(4), 457–467.

Hedjazi, S., & Razavi, S. H. (2018). A comparison of Canthaxanthine Pickering emulsions, stabilized with cellulose nanocrystals of different origins. *International Journal of Biological Macromolecules, 106*, 489–497.

Hosseini, M., Razavi, S., & Mousavi, M. (2009). Antimicrobial, physical and mechanical properties of chitosan-based films incorporated with thyme, clove and cinnamon essential oils. *Journal of Food Processing and Preservation, 33*(6), 727–743.

Jamróz, E., Juszczak, L., & Kucharek, M. (2018). Development of starch-furcellaran-gelatin films containing tea tree essential oil. *Journal of Applied Polymer Science, 135*(42), Article 46754.

Javanmardi, J., Stushnoff, C., Locke, E., & Vivanco, J. (2003). Antioxidant activity and total phenolic content of Iranian Ocimum accessions. *Food Chemistry, 83*(4), 547–550.

Karami, A., Kavoosi, G., & Maggi, F. (2019). The emulsion made with essential oil and aromatic water from Oliveria decumbens protects murine macrophages from LPS-induced oxidation and exerts relevant radical scavenging activities. *Biocatalysis and Agricultural Biotechnology, 17*, 538–544.

Keawchaoon, L., & Yoksan, R. (2011). Preparation, characterization and in vitro release study of carvacrol-loaded chitosan nanoparticles. *Colloids and Surfaces B: Biointerfaces, 84*(1), 163–171.

Khalil, H., Tye, Y., Saurabh, C., Leh, C., Lai, T., Chong, E., et al. (2017). Biodegradable polymer films from seaweed polysaccharides: A review on cellulose as a reinforcement material. *Express Polymer Letters, 11*(4).

Khan, M. R., & Sadiq, M. B. (2021). Importance of gelatin, nanoparticles and their interactions in the formulation of biodegradable composite films: A review. *Polymer Bulletin, 78*(7), 4047–4073.

Kilinc, D., Ocak, B., & Özdestan-Ocak, Ö. (2021). Preparation, characterization and antioxidant properties of gelatin films incorporated with Origanum onites L. essential oil. *Journal of Food Measurement and Characterization, 15*, 795–806.

Liu, J., Song, F., Chen, R., Deng, G., Chao, Y., Yang, Z., et al. (2022). Effect of cellulose nanocrystal-stabilized cinnamon essential oil Pickering emulsions on structure and properties of chitosan composite films. *Carbohydrate Polymers, 275*, Article 118704.
Lu, Y., Luo, Q., Chu, Y., Tao, N., Deng, S., Wang, L., et al. (2022). Application of gelatin in food packaging: A review. *Polymers, 14*(3), 436.
Luo, Y., Wu, Y., Wang, Y., & Yu, L. (2021). Active and robust composite films based on gelatin and gallic acid integrated with microfibrillated cellulose. *Foods, 10*(11), 2831.
Malihi, N., Danafar, F., & Moosavi-nasab, M. (2022). The effect of Oliveria decumbens Vent. essential oils and lysozyme on physicochemical and functional properties of fish gelatin film. *Journal of Food Measurement and Characterization, 16*(3), 2356–2364.
Martelli-Tosi, M., Masson, M. M., Silva, N. C., Esposto, B. S., Barros, T. T., Assis, O. B., et al. (2018). Soybean straw nanocellulose produced by enzymatic or acid treatment as a reinforcing filler in soy protein isolate films. *Carbohydrate Polymers, 198*, 61–68.
Mirahmad, A., Hafez Ghoran, S., Alipour, P., Taktaz, F., Hassan, S., Naderian, M., et al. (2024). Oliveria decumbens Vent. (Apiaceae): Biological screening and chemical compositions. *Journal of Ethnopharmacology, 318*, Article 117053.
Nikravan, L., Maktabi, S., Ghaderi Ghahfarrokhi, M., & Mahmoodi Sourestani, M. (2021). The comparison of antimicrobial and antioxidant activity of essential oil of Oliveria decumbens and its nanoemulsion preparation to apply in food industry. *Iranian Veterinary Journal, 17*(3), 78–87.
Onyeaka, P. O., Dai, H., Feng, X., Wang, H., Fu, Y., Yu, Y., et al. (2023). Effect of different types of nanocellulose on the structure and properties of gelatin films. *Food Hydrocolloids, 144*, Article 108972.
Oyeoka, H. C., Ewulonu, C. M., Nwuzor, I. C., Obele, C. M., & Nwabanne, J. T. (2021). Packaging and degradability properties of polyvinyl alcohol/gelatin nanocomposite films filled water hyacinth cellulose nanocrystals. *Journal of Bioresources and Bioproducts, 6*(2), 168–185.
Pastor, C., Sánchez-González, L., Chiralt, A., Cháfer, M., & González-Martínez, C. (2013). Physical and antioxidant properties of chitosan and methylcellulose based films containing resveratrol. *Food Hydrocolloids, 30*(1), 272–280.
Peña, C., De La Caba, K., Eceiza, A., Ruseckaite, R., & Mondragon, I. (2010). Enhancing water repellence and mechanical properties of gelatin films by tannin addition. *Bioresource Technology, 101*(17), 6836–6842.
Pereda, M., Aranguren, M. I., & Marcovich, N. E. (2010). Caseinate films modified with tung oil. *Food Hydrocolloids, 24*(8), 800–808.
Pirich, C. L., Picheth, G. F., Machado, J. P. E., Sakakibara, C. N., Martin, A. A., de Freitas, R. A., et al. (2019). Influence of mechanical pretreatment to isolate cellulose nanocrystals by sulfuric acid hydrolysis. *International Journal of Biological Macromolecules, 130*, 622–626.
Rivero, S., Garcia, M. A., & Pinotti, A. (2010). Correlations between structural, barrier, thermal and mechanical properties of plasticized gelatin films. *Innovative Food Science & Emerging Technologies, 11*(2), 369–375.
Robledo, N., Vera, P., López, L., Yazdani-Pedram, M., Tapia, C., & Abugoch, L. (2018). Thymol nanoemulsions incorporated in quinoa protein/chitosan edible films; antifungal effect in cherry tomatoes. *Food Chemistry, 246*, 211–219.
Rogovina, S., Aleksanyan, K., Prut, E., & Gorenberg, A. (2013). Biodegradable blends of cellulose with synthetic polymers and some other polysaccharides. *European Polymer Journal, 49*(1), 194–202.
Roy, S., & Rhim, J. W. (2021). Gelatin/agar-based functional film integrated with Pickering emulsion of clove essential oil stabilized with nanocellulose for active packaging applications. *Colloids and Surfaces A: Physicochemical and Engineering Aspects, 627*, Article 127220.
Saidane, D., Perrin, E., Cherhal, F., Guellec, F., & Capron, I. (2016). Some modification of cellulose nanocrystals for functional Pickering emulsions. *Philosophical Transactions of the Royal Society A: Mathematical, Physical & Engineering Sciences, 374*(2072), Article 20150139.
Saidi, M. (2014). Antioxidant activities and chemical composition of essential oils from Satureja khuzestanica, Oliveria decumbens and Thymus daenensis. *Journal of Essential Oil Bearing Plants, 17*(3), 513–521.
Shahiri Tabarestani, H., Sedaghat, N., Jahanshahi, M., Motamedzadegan, A., & Mohebbi, M. (2017). Development of optimized edible packaging based on white-cheek shark (Carcharhinus dussumieri) skin gelatin biopolymer: Mechanical, water vapor permeability, and structural properties. *Journal of Aquatic Food Product Technology, 26*(10), 1244–1258.
Shakila, R. J., Jeevithan, E., Varatharajakumar, A., Jeyasekaran, G., & Sukumar, D. (2012). Comparison of the properties of multi-composite fish gelatin films with that of mammalian gelatin films. *Food Chemistry, 135*(4), 2260–2267.
Shen, Y., Ni, Z. J., Thakur, K., Zhang, J.-G., Hu, F., & Wei, Z.-J. (2021). Preparation and characterization of clove essential oil loaded nanoemulsion and pickering emulsion activated pullulan-gelatin based edible film. *International Journal of Biological Macromolecules, 181*, 528–539.
Shi, W. J., Tang, C. H., Yin, S.-W., Yin, Y., Yang, X. Q., Wu, L.-Y., et al. (2016). Development and characterization of novel chitosan emulsion films via pickering emulsions incorporation approach. *Food Hydrocolloids, 52*, 253–264.
Souza, A. G.d., Ferreira, R. R., Aguilar, E. S. F., Zanata, L., & Rosa, D.d. S. (2021). Cinnamon essential oil nanocellulose-based pickering emulsions: Processing parameters effect on their formation, stabilization, and antimicrobial activity. *Polysaccharides, 2*(3), 608–625.
Tabaestani, H. S., Sedaghat, N., Pooya, E. S., & Alipour, A. (2013). Shelf life improvement and postharvest quality of cherry tomato (Solanum lycopersicum L.) fruit using basil mucilage edible coating and cumin essential oil. *International Journal of Agronomy and Plant Production, 4*(9), 2346–2353.
Tongnuanchan, P., Benjakul, S., & Prodpran, T. (2012). Properties and antioxidant activity of fish skin gelatin film incorporated with citrus essential oils. *Food Chemistry, 134*(3), 1571–1579.
Tongnuanchan, P., Benjakul, S., Prodpran, T., Pisuchpen, S., & Osako, K. (2016). Mechanical, thermal and heat sealing properties of fish skin gelatin film containing palm oil and basil essential oil with different surfactants. *Food Hydrocolloids, 56*, 93–107.
Wahyuningtyas, M., Jadid, N., Burhan, P., & Atmaja, L. (2019). Physical and chemical properties of gelatin from red snapper scales: Temperature effects. *Jurnal Teknik ITS, 8*(2), F95–F101.
Wang, H., Du, H., Liu, K., Liu, H., Xu, T., Zhang, S., et al. (2021). Sustainable preparation of bifunctional cellulose nanocrystals via mixed H2SO4/formic acid hydrolysis. *Carbohydrate Polymers, 266*, Article 118107.
Wang, H., Xie, H., Du, H., Wang, X., Liu, W., Duan, Y., et al. (2020). Highly efficient preparation of functional and thermostable cellulose nanocrystals via H2SO4 intensified acetic acid hydrolysis. *Carbohydrate Polymers, 239*, Article 116233.
Wulandari, W., Rochliadi, A., & Arcana, I. (2016). Nanocellulose prepared by acid hydrolysis of isolated cellulose from sugarcane bagasse. *Paper presented at the IOP conference series: Materials science and engineering*.
Yıldırım, A., Mavi, A., & Kara, A. A. (2001). Determination of antioxidant and antimicrobial activities of Rumex crispus L. extracts. *Journal of Agricultural and Food Chemistry, 49*(8), 4083–4089.